TESTING AND ANALYSIS OF LARGE CURVED GRID-STIFFENED COMPOSITE PANELS

Adam C. Biskner*, John E. Higgins**
***CSA Engineering, Inc., **Air Force Research Laboratory Space Vehicles Directorate**

Keywords: *composite, structure, grid-stiffened, failure analysis, fairing*

Abstract

A composite grid-stiffened structure was selected for the payload fairing of the Minotaur IV launch vehicle. During development the structural concept failed at substantially lower levels than originally expected. Various failure mechanisms were examined and joint peel-off failure was ultimately recognized as the controlling criterion for this structure. The identification of this failure mechanism and the assessment of bounding strains to control it, required extensive test and analysis effort. As such the final fairing design incorporated an undesirably thick skin to reduce the strain between the skin and ribs. This project investigated a means of preventing joint peel-off failure by integrating lightweight foam inserts between the stiffeners on the interior of the fairing. Thorough empirical and analytical results are presented that indicate the reinforcing foam can be utilized to sufficiently stabilize the joint thus preventing peel-off failure and increasing the load carrying capability while maintaining the system's mass.

1 Introduction

The Air Force Research Laboratory continues to develop new spacecraft and launch vehicle structures in an effort to enhance the performance and cost effectiveness of future Air Force missions. In particular composite structures have received considerable developmental attention due to their superior stiffness and strength-to-weight ratio characteristics. In recent years a new carbon fiber composite fairing was developed for the Minotaur IV launch vehicle. The IM7/977-2 fairing consists of a laminate skin co-cured to a reinforcing Advanced Grid-Stiffened (AGS) rib structure, shown in Fig. 1. Compared to previous designs, this concept is lighter weight and requires reduced manufacturing costs [1].

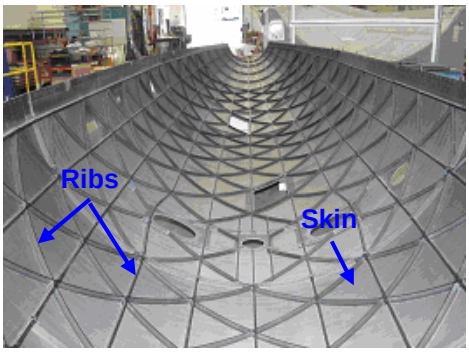

Fig. 1. Interior of the Minotaur fairing

At the outset of the Minotaur fairing development, global buckling instability was assumed to be the controlling factor in the design process; however, substructure test panels demonstrated early failure. Extensive efforts were made to identify the failure mode. Ultimately joint peel-off strain was determined to be the controlling criterion [2]. Joint peel-off is caused by relative rotation of the skin and ribs structures and is evaluated with the Strain Invariant Failure Theory (SIFT) [3]. To minimize the weight of the fairing, the skin pockets are allowed to displace causing localized non-linear buckling behavior. As a result of the skin buckling patterns, a bending moment forms in the skin that tends to peel it from the AGS, inducing local failure. Once delamination initiates locally, the crack quickly propagates along the entire joint between the skin and stiffener structure, leading to global failure of the fairing. To prevent joint peel-off, an undesirably thick skin detail was incorporated on the launch vehicle. The objective of this study was to investigate a means of stabilizing the skin/rib interface without increasing the system mass of the fairing.

Several alternative means of stabilizing the T-joint were investigated. These designs were initially examined, both analytically and experimentally, on a material, coupon, and sub-scale level. The research was continued on a sub-structure basis for one beneficial design option.

2 Flat Panel Study

Three viable design concepts that inherently prevented rotation at the skin/rib interface were developed and tested. Initially, the alternative concepts were designed on an equal mass basis with a baseline representation of the current Minotaur fairing and evaluated for strength. The new designs were: 1) Rohacell Reinforced, 2) Carbon Foam Reinforced, and 3) Skinless.

The first concept leveraged thinner skin architecture in order to allow for the mass of Rohacell, a closed cell structural foam, to be incorporated into the areas between the grid stiffeners on the interior side of the panel. The foam inserts, which were bonded in place with Hysol 9309, were intended to dampen skin/rib rotation. The second alternative further reduced the skin thickness and carbon foam was introduced to reinforce the AGS. Contrary to the first concept, the carbon foam portion of this panel functioned as the exterior surface of the design to serve the vehicle's Thermal Protection System (TPS). Integrating the TPS into the structure increased the mass allowance, which was this concept's primary design advantage. Alternative three was a departure from the Carbon Foam Reinforced design that did not contain a carbon fiber composite skin. Instead the AGS was supported solely by a carbon foam panel. By completely removing the skin, more carbon foam could be used to support the rib structure.

2.1 Flat Panel Experimental Setup

A three phase experimental plan was performed to evaluate the design alternatives. Phase one investigated the compressive strength's and stiffness's of the two foams. Next, T-specimen coupons were produced to examine the pull-off strength between the skin and AGS grid for each skin configuration in the second phase. This information was needed to determine the allowable peel-off strain for each of the skin/rib configurations. The final experimental stage was to manufacture integrated test panels that represented the three alternatives as well as a forth panel that emulated the nominal or Baseline fairing configuration and load them in compression until ultimate failure was reached. This portion of the study was an initial investigation into methods to stabilize the skin/rib interface, as such existing tooling was used to minimize the cost of the experiment which dictated the AGS configuration. Although the grid pattern was not consistent with that of the operational Minotaur fairing, this test offered a relative comparison between the various designs. The failure load of each alternative design was compared to that of the baseline panel to evaluate the effectiveness of the new concept. In addition to the panel's load response, opposing strain gages were mounted in the middle of the center axial rib to analyze the stiffener's out-of-plane buckling behavior. The flat panel compression test setup is shown in Fig 2. A divergence in the strain gage responses indicates the rib is rotating in a manner that induces peel-off failure.

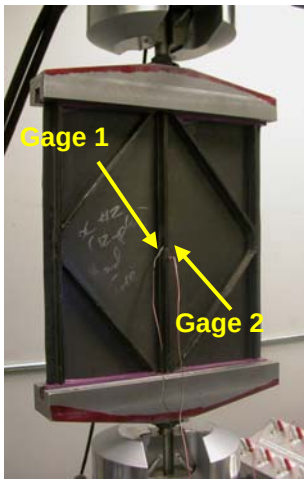

Fig. 2. Flat panel test setup

2.2 Flat Panel Experimental Results

The purpose of phase one was to evaluate the compressive strength of two foams, closed cell Rohacell with a density of 75 kg/m^3 and carbon foam with a 275 kg/m^3 density. The results are shown in Fig. 3. The Rohacell foam displayed an average ultimate compressive strength of 224 psi. The maximum load was typically realized at a strain of 0.09 in/in and could be maintained by the material until a strain of 0.70 in/in. The carbon foam had an average maximum compressive strength of 663 psi, which occurred at a strain of 0.13 in/in. The specific weight of the carbon foam was 3.7 times heavier than that of the Rohacell foam, but the average compressive strength was less than three times greater, meaning the Rohacell foam had a more impressive strength-to-weight ratio. The Cfoam concepts were not discarded from the evaluation process due to the material's lower strength/weight ratio because the alternatives that included Cfoam had an added advantage of incorporating the weight of the TPS into the structural system which reduced the weight penalty of the material.

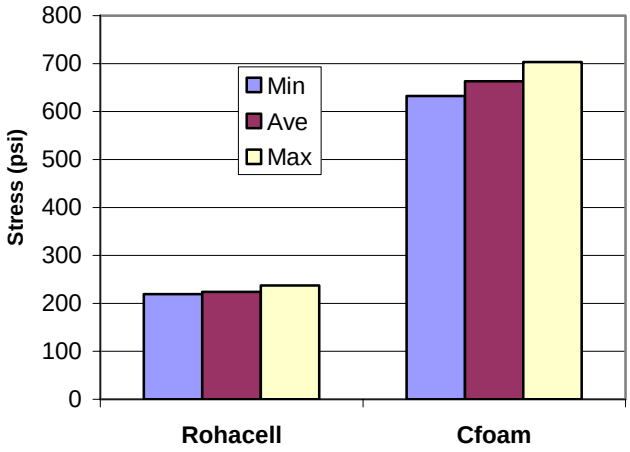

Fig. 3. Foam material compressive strengths

Through a process that involves applying the results of the pull-off tests performed in the second experimental phase as boundary conditions in a solid Finite Element Method (FEM) model, the allowable J1 value for each skin thickness was determined [4]. These results are shown in Fig. 4. Although three discrete skin thicknesses were incorporated into the different design alternatives, the panel testing determined failure criterion data was needed only for the 8 and 12-ply skin lay-ups.

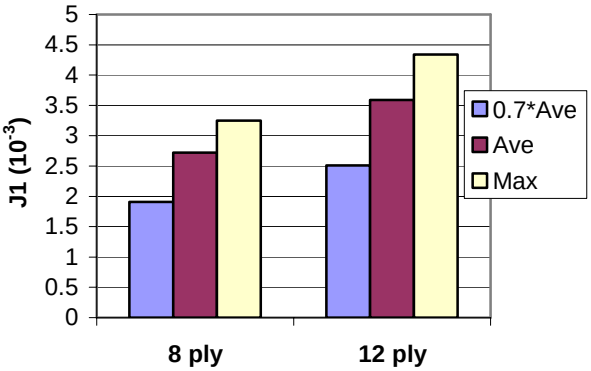

Fig. 4. J1 values from T-specimen experiment

The results of the panel compression test identified that only the Rohacell Reinforced concept outperformed the baseline's strength. Additionally, Fig. 5 displays the two panel's strain gage data and demonstrates that the reinforced panel sufficiently prevented rib rotation compared to the baseline test article while increasing the compressive strength by 35 percent.

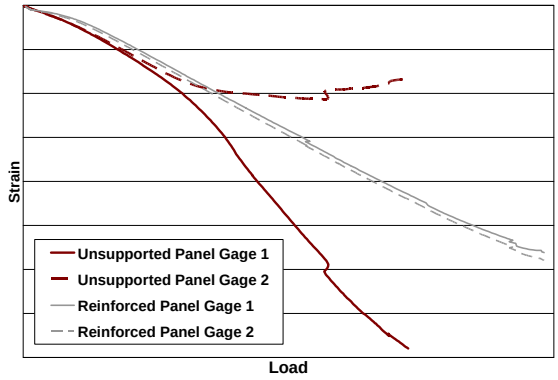

Fig. 5. Strain gage responses of two flat panels center ribs during the compression test

2.3 Flat Panel Analysis

Finite element analysis was required to further study the empirical results. Only the top performing alternative concept and the baseline architecture were analyzed. The panel model was constructed of shell elements to analyze its material and structural behavior at failure. At the conclusion of the simulation, nodal reaction loads from the skin region near the joint were compiled and applied to a refined two-dimensional solid model of the joint geometry. The solid elements determined the value of J1 present in the panel, this process is described in detail in Biskner (2005). Fig. 4 displays the Baseline panel's J1 response for each discrete location along the skin/rib interface.

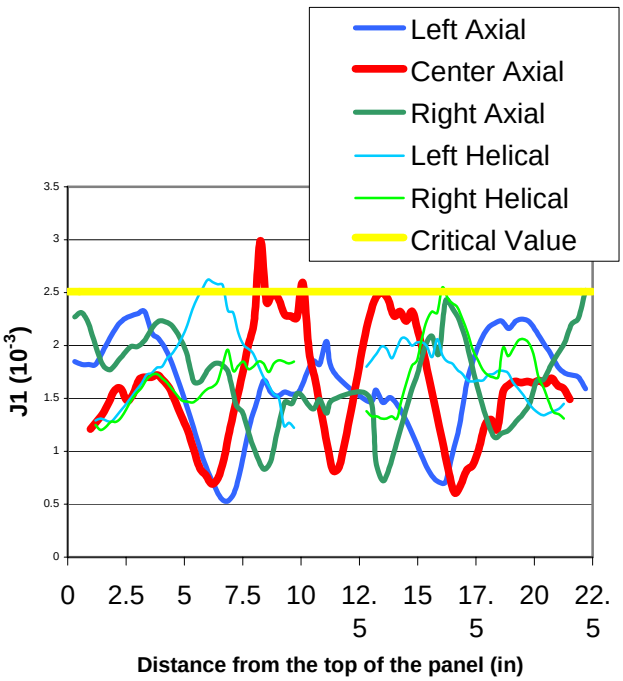

Fig. 6. Baseline panel J1 response

The simulations determined the baseline panel's first strain invariant exceeded the critical value only in the locations where the test panel experienced delamination, indicating that joint peel-off was the failure mode. Conversely, the strain invariant values in the reinforced panel did not approach the allowable limit. This study found that the highest strain invariant present in the Rohacell Reinforced panel was less than one percent of the allowable value. The foam increased the strength of the panel and prevented joint peel-off failure.

Fig. 7 displays a contour plot of the (a) Baseline and (b) Rohacell Reinforced panels displacements superimposed on their deformed shape. The foam inserts are hidden in the Rohacell Reinforced plot so the skin behavior is visible. The Baseline panel exhibited local skin and rib buckling, whereas the Rohacell Reinforced panel did not experience any visible local buckling. Instead, it buckled globally about a hinge in the center of the panel. The strain gage data from the flat panel test suggested that the foam sufficiently reinforced the center rib, the analysis results convey that the foam improved the overall response of the panel.

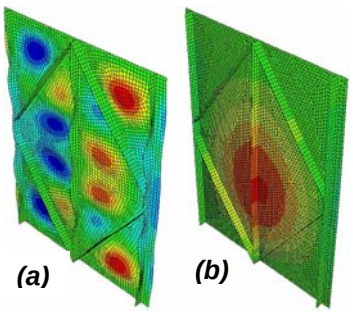

Fig. 7. Displacement contours of the (a) baseline and (b) reinforced panels

After the J1 analysis, three additional failure modes were examined: joint pull-off, joint shear, and structural buckling. Joint pull-off is a grid-stiffened structure failure mode common in designs with thick skin that have a high bending stiffness. The Rohacell Reinforced panel did not have a thick skin, but the combined properties of the eight ply skin and the Rohacell foam created a stiff skin. Pull-off failure occurs when the tensile strength of the adhesive layer between the skin and rib structures is exceeded. The section forces from the rib elements were collected to determine the normal stresses pulling the rib off the skin. Joint shear failure occurs when the shear capability of the adhesive is exceeded as the shear force is passed from the rib structure to the skin detail. In both cases only a small fraction of the allowable stress was realized.

The panel models were then modified to conduct a buckling analysis by applying rotational constraints to the AGS grid which forced the stiffeners to buckle in the plane perpendicular to the skin's original plane. Each model was compressed by an applied displacement until the structure buckled globally. The final compressive load was regarded as the structure's maximum load carrying limit. The non-reinforced Baseline panel achieved only a small fraction of its buckling limit; whereas the Rohacell Reinforced panel realized 85 percent of its theoretical buckling load. The conclusion of this analysis is that structural buckling was the controlling factor in the foam-reinforced concept.

3 Large Curved Panel Study

The results of the flat panel study motivated further investigation with large curved panels, a test article containing greater fidelity to an operational fairing. The panels were 42 inches tall and represented approximately a 30º arc of a 61 inch diameter cylinder. The greatest improvement in consistency with the operational fairing was fabricating new tooling that produced the same AGS grid as the Minotaur which can be seen by comparing Fig. 2 to Fig 8. As in the flat panel study, large curved test articles were only fabricated for the 12-ply skin baseline representation of the fairing and the 8-ply skin with a Rohacell Reinforced AGS structure.

3.1 Curved Panel Experimental Setup

The objective of the test was to evaluate the relative axial compression strengths of the two types of panels while preventing global buckling of the panel caused by the free vertical edges. To accomplish this goal, the initial phase of the test program was to design and manufacture a suitable test fixture.

Fig. 8 shows a curved Baseline test article in the fixture designed and fabricated for edgewise compression testing. Both the top and bottom fixtures were composed of two steel plates. The cross-sectional dimensions of all plates were 2 inches x 6 inches. A shorter 22 inches connector plate attached to the load cell (top) or actuator (bottom) and transmitted the applied load to the longer 38 inches loading plate. The locations of the load transmission points between the two steel plates were chosen to minimize the bending of the longer loading plates when testing the curved panels.

To provide a means of adjusting the load distribution within the curved test panel, a series of four alignment bolts were installed in the shorter connector plate of the bottom test fixture. Tightening of a particular bolt provided an additional upward displacement to the loading cylinder that contacted the loading plate. Using these four alignment bolts, it was possible to provide both front-to-back and left-to-right adjustments to the load distribution of the test panel.

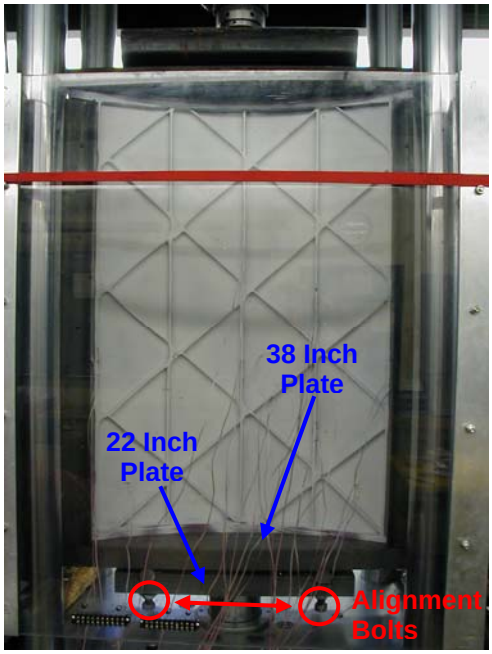

Fig. 8. Curved panel test setup

During compression testing, the vertical boundaries of the curved panels were required to be supported in such a manner that the panel would not experience radial buckling. Additionally the edge supports used to prevent buckling were required to not produce local failure. To satisfy these requirements I-beam clamp supports, shown in Fig. 9, were designed and fabricated. Each support consisted of two steel I-beams connected using a series of attachment bolts. A steel plate was inserted between two I-beams to form a clamping device which could be secured onto the edge of the test panel by tightening the attachment bolts. The flange of each I-beam that was to contact the panel during testing was machined to produce a smooth, planar edge that provided a uniform support along the length of the panel. When installed onto the test panel, each edge support rested on the base plate of the bottom test fixture.

Fig. 9. Vertical edge test fixture

Twenty-four channels of data were collected during the experiment. Two channels were used to measure the axial displacement of the test setup with LVDT sensors, four uniaxial strain gages were used to quantify the uniformity of the load across the width of the panel, and 18 strain channels were used to evaluate the panel's performance. The gage locations are shown in Fig. 10.

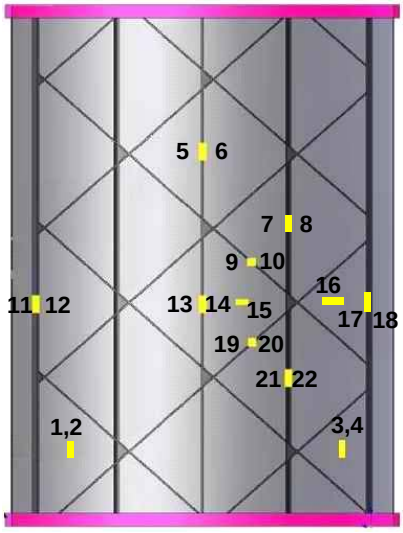

Fig. 10. Curved panel strain gage locations

Prior to testing the panels were spray painted white to help visually identify failure locations. The test articles were also prepared by potting the top and bottom edges in epoxy to prevent end crushing. Once the panels were potted, the surfaces required additional machining to obtain the flatness and parallelism to one another, as well and perpendicularity to the axial ribs. To machine the panel ends, a wooden fixture was constructed and clamped to the mill. The potted ends were milled to a depth that resulted in the end of the carbon panel being visible along the entire length of the potted edge. This setup is shown in Fig. 11. Once this step was completed, the panel was positioned into a four-post MTS servo hydraulic load frame. The test

setup and execution was preformed by Alveus Engineering.

Fig. 11. Curved panel on milling machine

3.2 Curved Panel Experimental Results

The structural testing exhibited that the Rohacell Reinforced panels failed under an average axial compression load of 81 kips. The 12-ply non-reinforced panels withstood an average load of 57 kips, 37 percent less than the reinforced version. This conclusion is very similar to the 35 percent advantage demonstrated by the Rohacell Reinforced flat panel relative to the Baseline flat panel. Due the changes in the test setup, the similarity of the reinforced concepts relative performance was not expected and is believed to be coincidental.

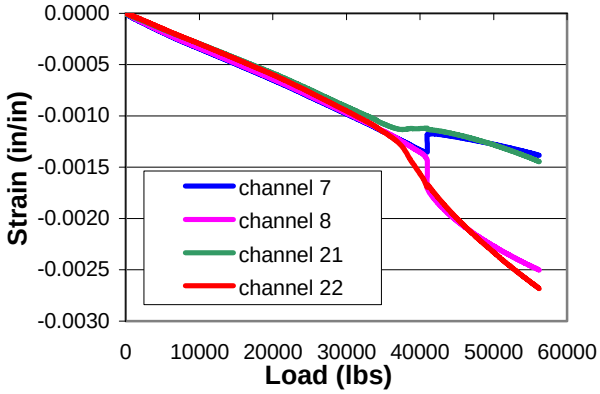

Fig. 12. Strain gage response on a Baseline curved panel of an axial rib

Fig. 12 displays the forth axial rib's strain gage responses of a typical Baseline curved panel during compression testing. The two pairs of opposing strain gages indicate the rib remained in plane until approximately 40 kips was applied before rotating out of plane. The strain data continued to diverge until ultimate failure was reached near 57 kips. Conversely, Fig. 13 demonstrates the strain data on the center axial rib of a Rohacell Reinforced panel remained consistent through the entire load ranch until the panel buckled globally under an applied load just less than 80 kips. This is strong evidence that the Rohacell inserts satisfactorily reinforced the AGS grid and prevented peel-off failure.

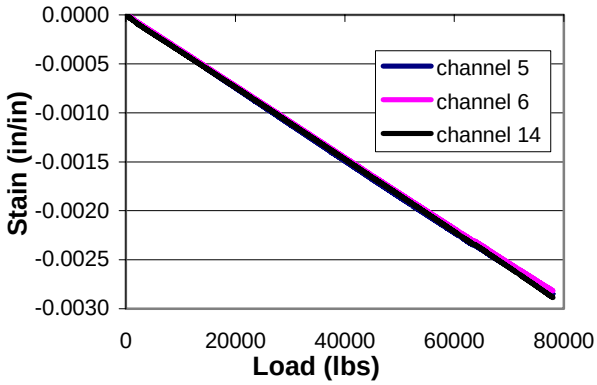

Fig. 13. Center axial rib strain gage response on a Rohacell Reinforced curved

At the conclusion of the testing, the degree to which the test procedure and fixtures met the experimental objectives was evaluated. Fig. 14 demonstrates the load distribution strain gages indicated each of the test articles carried the compression load uniformly until local buckling began to occur, approximately 35 kip in the case shown here. Also, the structural failure was initiated by buckling in the center of the panel versus simply folding the panel about a center hinge, this result is displayed in Fig. 15. Both results suggest the test setup successfully accomplished its purpose.

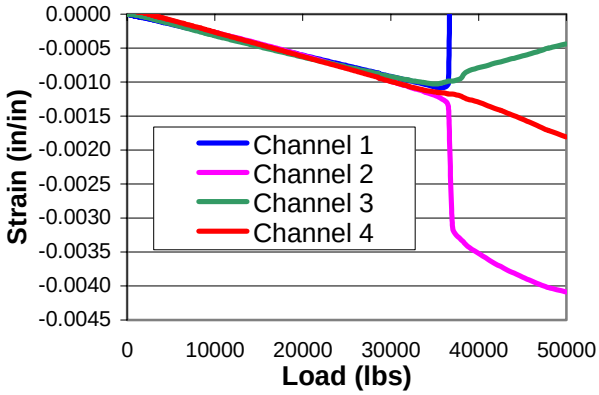

Fig. 14. 12-ply panel load uniformity strain data

Fig. 15. Failed curved panel

3.3 Curved Panel Analysis

Fig. 16 demonstrates the stress contour for (a) the Baseline panel, and (b) the foam reinforced panel. The two images display the panels Von Mises stress superimposed on the shape of the deformed panels, the deformations are amplified 20X to make them visually noticeable. The foam components of image (b) were hidden to display the response of the composite panel. This modeling effort is currently in-progress, however, the deformed shapes in these initial results indicate the reinforcing foam sufficiently stiffens the skin and reinforces the rib structure to delay peel-off failure. Additionally, the Baseline non-reinforced panel allowed rotation of both the skin and rib architectures which is conducive to peel-off failure. These same results were demonstrated in the flat panel testing and analysis, and the curved panel compression experiment.

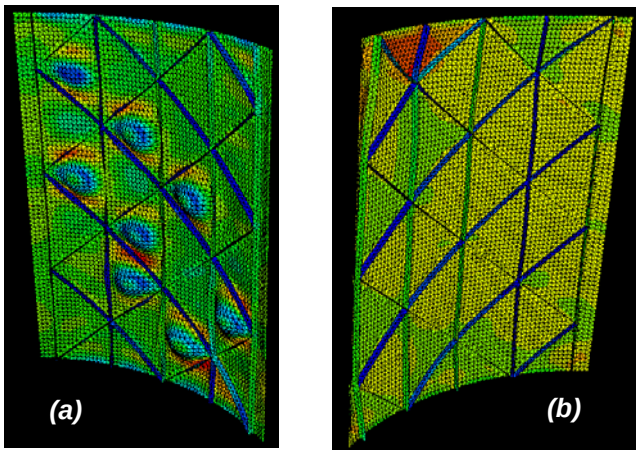

Fig. 16. Initial curved panel FEM results

4 Conclusions

Composite AGS structures are a valuable technology to the US Air Force. A fairing for the Minotaur IV launch vehicle was developed that utilized this advanced structural technique. The fairing required an undesirably thick skin to prevent peel-off failure between the skin and rib components, thus increasing its mass. This study has shown Rohacell is capable of stabilizing the AGS skin-to-rib interface hence preventing peel-off failure without increasing the mass of the structure. This conclusion has been rigorously demonstrated through progressive levels of testing and analysis. The data reported in this paper provides reasonable evidence that the an optimized Rohacell Reinforced AGS design could meet the requirements of a structure such as the Minotaur IV fairing at a reduced mass compared to the current composite AGS shroud.

Acknowledgments

The authors would like to thank Greg Sanford of CSA Engineering, Inc. for providing experimental and modeling guidance during this study as well as Dan Adams of Alveus Engineering for designing and administering the curved panel compression test.

References

[1] Higgins J., Wegner P., Van West B., Viisoreanu A. “Post Buckling Test Response and Analysis of Fiber Composite Grid-Stiffened Structures” *Proceedings of 43rd AIAA SDM Conference*, Denver, CO, AIAA 2002-1332, 2002.

[2] Higgins J., Wegner P., Viisoreanu A., Sanford G. “Design and Testing of the Minotaur Advance Grid-Stiffened Fairing”. *Composite Structures*, Vol. 66, pp 339-349, 2004.

[3] Gosse J., “Strain Invariant Failure Theory Criteria for Polymers in Composite Material” *Proceedings of 42nd AIAA SDM Conference*, Seattle, WA, AIAA 2001-1184, 2001.

[4] Biskner A., Higgins J., “Design and Evaluation of a Reinforced Advanced Grid-Stiffened Composite Structure” *Proceedings of 46rd AIAA SDM Conference*, Austin, TX, AIAA 2005-2153, 2005.